Spinning of Poly(ethylene terephthalate) Fibers Filled with Inorganic Fillers

Boonsri Kusuktham

Division of Textile Chemical Engineering, Faculty of Textile Industries, Rajamangala University of Technology Krungthep, Bangkok 10120, Thailand

Received 17 June 2011; accepted 13 December 2011
DOI 10.1002/app.36656
Published online in Wiley Online Library (wileyonlinelibrary.com).

ABSTRACT: Poly(ethylene terephthalate) (PET)/inorganic fillers were prepared by a melt-spinning method, and their morphologies and properties were investigated. Four inorganic fillers were studied and compared: calcium carbonate, calcium silicate, magnesium hydroxide, and silica fume. All of the fillers were modified with vinyltriethoxysilane (VTES) in diethyl ether at room temperature for 24 h. The modification of these fillers with VTES improved their agglomeration, hydrophobicity, and heat-resistance properties. Also, the incorporation of the fillers into the PET fibers increased their thermal resistance. The factor effecting the thermal degradation of the PET fibers was the type of filler. © 2012 Wiley Periodicals, Inc. J Appl Polym Sci 000: 000–000, 2012

Key words: composites; fibers; fillers; polyesters

INTRODUCTION

Poly(ethylene terephthalate) (PET) is used in a wide array of fields, both in fiber and nonfiber applications (e.g., packing, electrical, automotive, construction). Polyester fiber is commonly used in the textile industry. The advantages of polyester fiber include its high crystallinity, strength, and tenacity. These properties have encouraged its application in industrial areas. However, PET is not thermally stable.

Inorganic fillers have been widely used in polymeric materials. For example, $CaCO_3$,[1,2] metal hydroxides,[3] and silane-based additives[4,5] have all been important in the development of materials. The heat resistance of these fillers has been examined. However, the differences in their thermal properties have not been reported. These fillers are as follows.

First, calcium carbonate (CC) is a common substance found in rock and is the main component of shells of marine organisms. It comprises polymorph aragonite and calcite. The main use of CC is in the construction industry. It is also used as an extender in paints and as a filler in plastics. Polypropylene compounds were filled with CC to increase rigidity.[6] Elleithy et al.[7] reported that high-density polyethylene (HDPE)/CC composites had better thermal stability than neat HDPE. In addition, the reinforcement of HDPE with CC increased its impact strength.[8]

Second, calcium silicate (CS) is obtained by the reaction of calcium oxide with silica at various ratios. CS is a white powder with a low bulk density and a high physical water absorption. It is used in roads, insulation, and bricks.[9]

Third, magnesium hydroxide (MH) is an inorganic compound. It is formed by precipitation of the metathesis reaction between magnesium salts and sodium, potassium, or ammonium hydroxide. Solid MH has smoke-suppressing and fire-retarding properties.[6] Fei et al.[3] found that MH improved the flame retardancy of polyamide 6.

Finally, silica fume (SF) is a byproduct of the production of silicon metal or ferrosilicon alloys. The polar surface of SF likes to absorb moisture, which induces the agglomeration of particles. It can be used in a variety of cementitious products, including concrete and mortars, as well as elastomer, polymer, and rubber applications.[10] It increased the thermal stability and charred residue of polypropylene.[11] Also, SF acted as a nucleating agent and increased the crystallization rate of poly(butylene succinate).[12] However, the hydrophilic character of these fillers induces their incompatibility with hydrophobic polymeric matrices.

Surface-modifying agents are used to coat the surfaces of filler materials to improve the interactions between the filler and the polymer matrix. The

Correspondence to: B. Kusuktham (kuboonsri@yahoo.com).

Contract grant sponsors: National Science & Technology Development Agency.

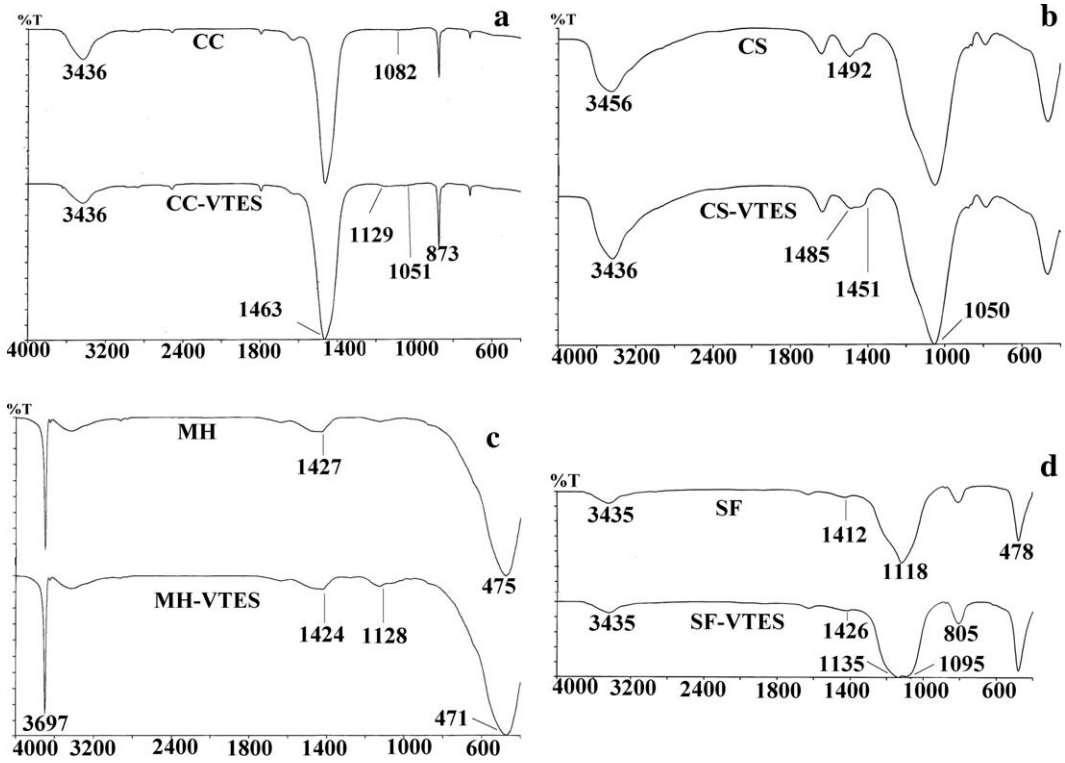

Figure 1 FTIR spectra of the unmodified and modified fillers: (a) CC, (b) CS, (c) MH, and (d) SF.

most common type of silane is alkoxysilane with the general molecular form $(RO)_3$—Si—R′—X, where X is an organofunctional group (e.g., amino, epoxy, methacrylate), R′ is typically a small alkylene linkage, [e.g., —$(CH_2)_n$—] between silicon and the organofunctional group, and RO is a hydrolyzable group, typically, methoxy, ethoxy, or acetoxy, which reacts with water to form silanol (Si—OH) and ultimately forms an oxane (Si—O—metal) bond with the inorganic substrate. Silanes may react with the filler surfaces after their alkoxy-functional groups have been hydrolyzed to form the corresponding silanol. Their silanol species may react with the hydroxy-functional groups on the surface of the filler and also with neighboring molecules. Consequently, a polysiloxane network is formed at the filler surface. It helps to change the filler surface properties. To derive the maximum benefit from the fillers, several factors must be considered, including the particle size, aspect ratio, and filler shape. The interfacial compatibility of the filler is also important and will assist in the dispersion and help minimize macrodefects in parts that can cause embrittlement.

Some synthetic polymers for fiber production are made by a melt-spinning process. The production steps as follows. First, polymer chips are dried and then melted. Next, the polymer melt is transported under pressure to spinning blocks, where an exact metering pump (e.g. a gear pump) maintains a highly even issue of the melt. The polymer melt is then forced through a fine filter. After filtration, the melt is forced through capillaries in a plate, called the *spinneret*, and in this way, an endless, fine stream of fluid is formed. Finally, the filaments are then quenched and solidified in the quench chamber while being drawn off from the bottom. A monofilament is produced at relatively low spinning speeds. This helps to reduce heat accumulation. The filament is usually quenched by passage into cold water or onto a cold quench roll immediately after extrusion; drawing is done either separately or inline.

In this research, PET fibers were produced by a melt-spinning method. PET is stable enough at temperatures above its melting point or softening point to be extruded in the molten state without substantial degradation. In addition, melt spinning is the most economical compared to all spinning processes. The aim of this research was to incorporate modified inorganic fillers into PET fibers. Also, the effects of these fillers on the thermal properties were compared. The addition of modified inorganic fillers to the PET fibers improve their thermal properties. These modified fibers could be used as thermal-resistance fibers.

This study was carried out to modify fillers such as CC, CS, MH, and SF with vinyltriethoxysilane (VTES). The melt blending of PET and the modified fillers was carried out in a single-screw extruder (Thailand). Specifically, the melt spinning of PET fibers filled with 1% of these fillers (by weight of the polyester chips) at a temperature of 265°C was

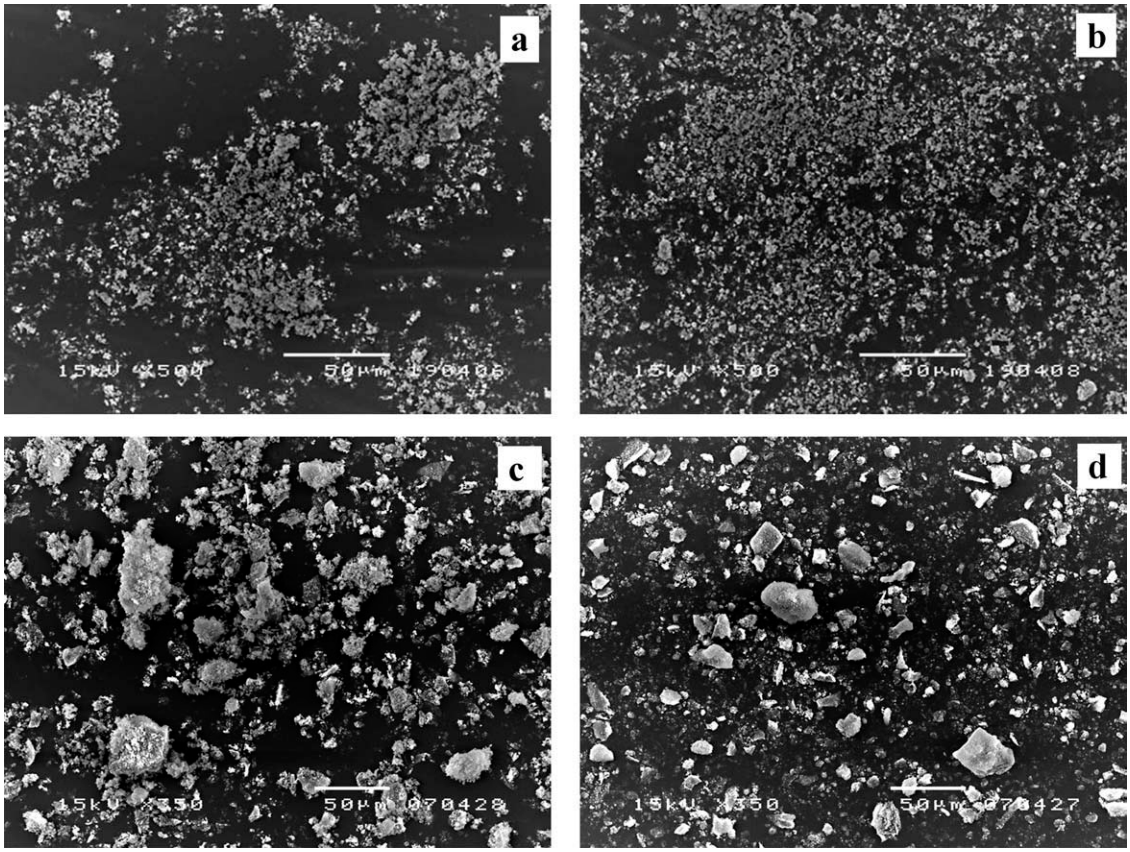

Figure 2 SEM micrographs of the unmodified and modified fillers: (a) unmodified CC, (b) modified CC, (c) unmodified CS, and (d) modified CS.

conducted. Also, their morphologies and thermal properties were investigated, and a comparison was done between fiber composites with four different fillers.

EXPERIMENTAL

Materials

CC, CS, and MH were purchased from Fluka (Singapore). SF was purchased from Wacker (Thailand). The PET chips were supplied by Thai Toray Synthetic Co, Ltd., (Thailand) in the form of bright PET chips (with no addition of TiO_2). The PET chips had an intrinsic viscosity of 0.639 dL/g and a density of 1.38 g/cm^3, with a weight-average molecular weight of 20,000. VTES was purchased from Aldrich (Singapore) and was used as received.

Surface treatment of the fillers with VTES

VTES (2% v/v) in diethyl ether was applied onto the surface of the fillers (4 g). The mixture was reacted at room temperature for 24 h. The dried fillers were washed with diethyl ether three times, dried at a temperature of 110°C for 2 h, and subsequently cooled in a desiccator.

Preparation of the PET/filler composites

The PET/filler composites were prepared in a Rajamangala University of Technology Krungthep laboratory-scale melt mixer. The melt blending of the PET and fillers was carried out in a single-screw extruder (Thailand) for 10 min. The fillers were 1 wt % of PET. The temperature in the mixer was 265°C, and the final composites extruded were cooled inline in a water bath, dried, and granulated.

Laboratory spinning of the PET into filaments

PET with or without fillers was spun with an equipment in the laboratory scale. A Rajamangala University of Technology Krungthep laboratory-scale melt spinning unit was employed for this study. Before spinning, the polymer chips were dried being heated at a temperature of 110°C for 8 h. The molten polymer was forced through a single-hole spinneret with a capillary diameter of 0.5 mm. The conditions of spinning were kept at a constant temperature of 265°C and a spinning speed of 200 m/min. The quenching of the filament was achieved in ambient air. The as-spun, undrawn filament was then collected.

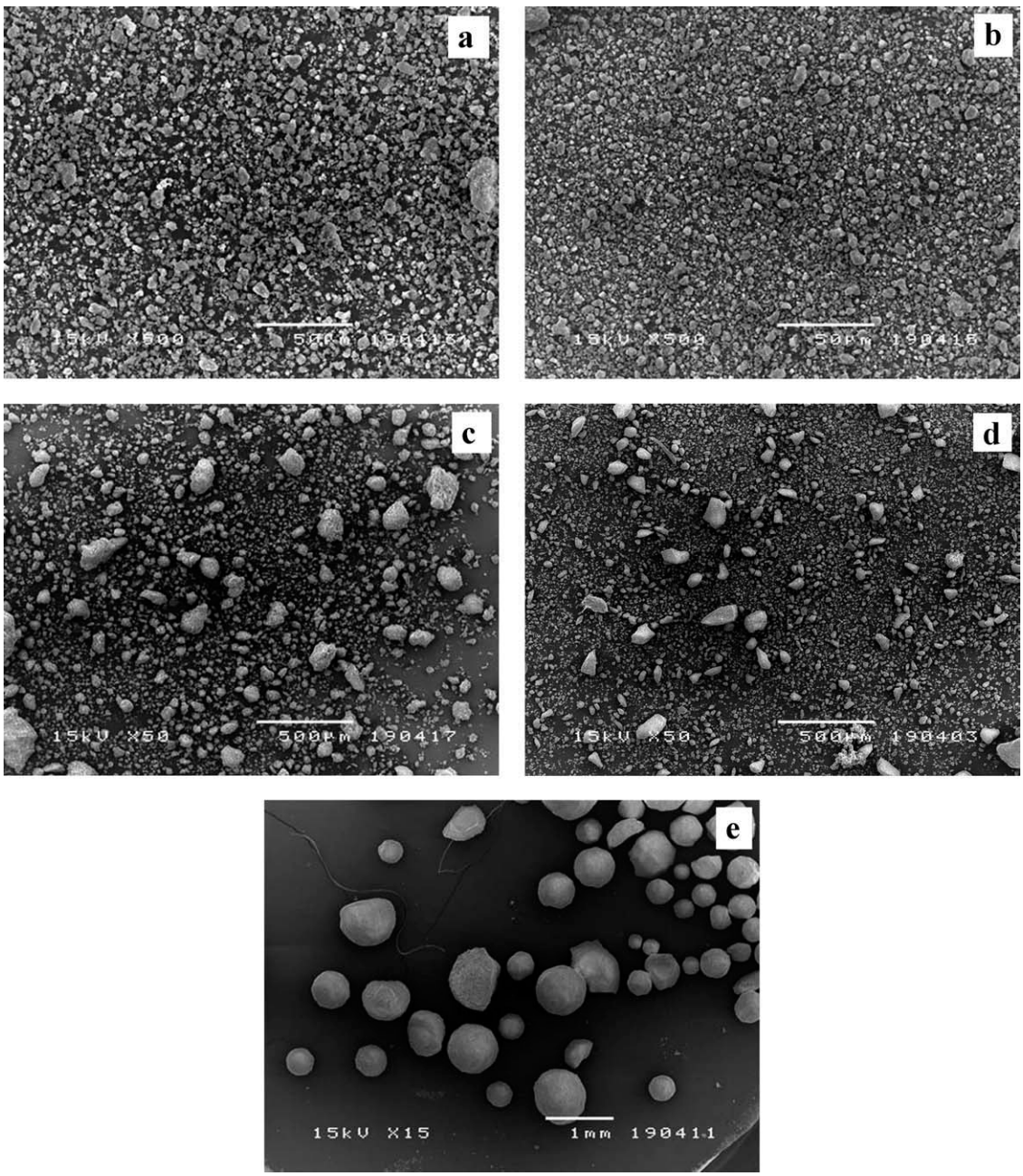

Figure 3 SEM micrographs of the unmodified and modified fillers: (a) unmodified MH, (b) modified MH, (c) unmodified and milled SF, (d) modified and milled SF, and (e) modified and no milling SF.

Characterization

Particle size measurement

The particle size distributions of the fillers were examined by a laser particle size distribution Mastersizer S long bed (version 2.19, Malvern Instruments, Ltd., Worcestershine, England).

Fourier transform infrared (FTIR) measurement

For the filaments, the specimen was cut into pieces less than 1 mm long. Then, the sample (1–3 mg) was mixed with KBr (200 mg) and pressed under pressure (8 MPa) for 5 min. For the fillers, it was also mixed with KBr and pressed under pressure. The FTIR spectra of the PET filaments and fillers were recorded with a PerkinElmer FTIR spectrophotometer system 2000 (Waltham, Massachusetts, United States of America) between 4000 and 370 cm^{-1}.

Morphology

The specimens were coated with gold in a Hitachi E102 ion sputterer. The surface morphologies of the fillers and PET fibers were observed with scanning

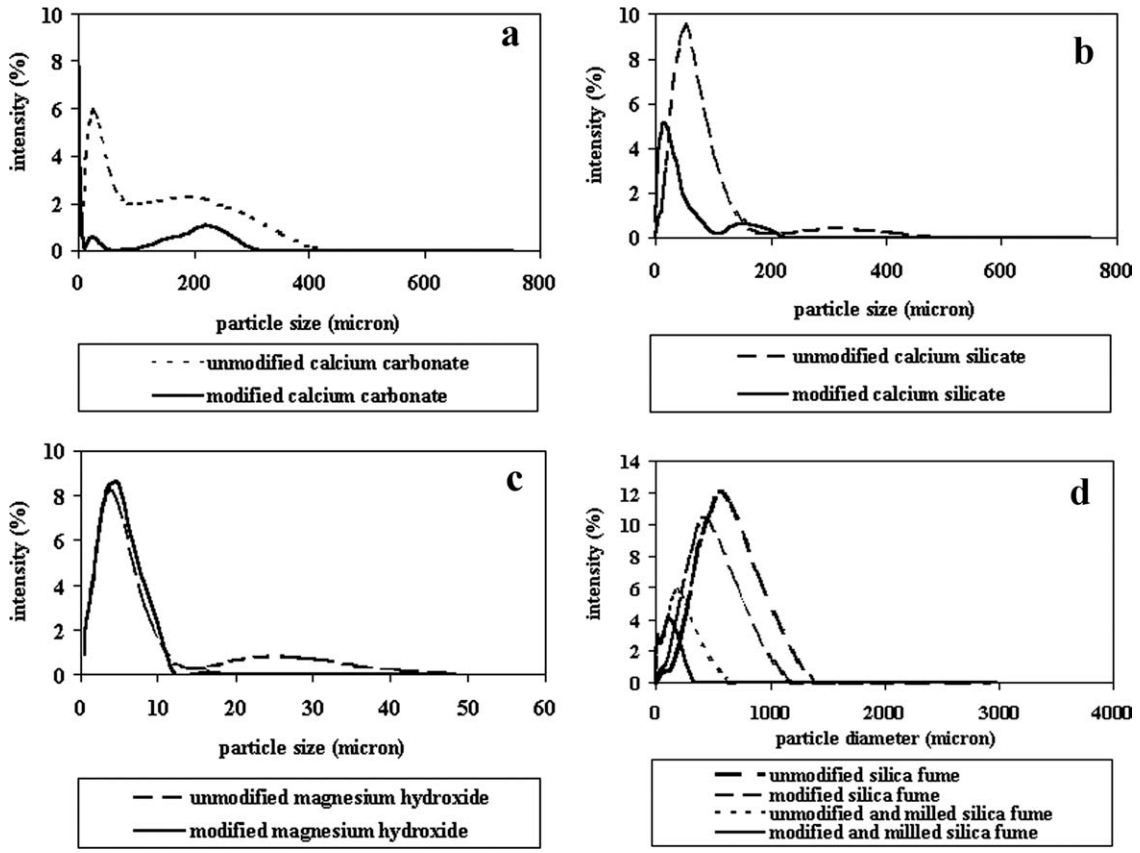

Figure 4 Particle size distribution of the unmodified and modified fillers: (a) CC, (b) CS, (c) MH, and (d) SF.

electron microscopy (SEM; JEOL JSM-5410LV, Tokyo, Japan) with an accelerating voltage of 15 kV.

Thermogravimetric analysis (TGA)

TGA was carried out with a Netzsch simultaneous thermal analyzer STA 409 C Jupiter (Burlington. Maryland, United States of America), which recorded the mass change as a function of temperature. The fiber was cut to approximately 1–2 mm in length, and a 17 ± 3-mg sample was analyzed under a nitrogen atmosphere from room temperature to 800°C at a heating rate of 20°C/min. In addition, the fillers were characterized under the same conditions.

RESULTS AND DISCUSSION

Surface modification of the fillers

Most filler materials have different physical properties compared to the polymers; for example, fillers usually have a polar surface that often must interact with nonpolar polymer matrices. Consequently, the weakest point in a filled composite is often at the PET–filler interface. Interactions between the PET and fillers, such as CC, CS, MH, and SF, may be enhanced with a filler-surface-modifying agent.

These fillers were modified with VTES. VTES is an organosilicone compound showing a $(CH_3{-}CH_2{-}O)_3{-}Si{-}CH{=}CH_2$ structure. Alkoxide groups on the silicon were hydrolyzed to silanols. In addition, the silanols condensed with each other to give a siloxane bond. The reactions are shown later.

Hydrolysis reaction

$$-Si-O-CH_2CH_3 + H_2O \rightarrow -Si-OH + CH_3CH_2OH \quad (1)$$

Condensation reaction

$$-Si-OH + -Si-OH \rightarrow -Si-O-Si + H_2O \quad (2)$$

VTES could react with the filler surfaces after its ethoxy functional group was hydrolyzed to form the

TABLE I
Thermal Degradation of the PET Fiber and PET Fiber Composites

Sample	PET	PET/CC	PET/CS	PET/MH	PET/SF
Onset temperature (°C)	414.6	418.8	415.2	418.1	415.3
Residual (wt %)	15.25	15.65	16.36	19.01	19.31

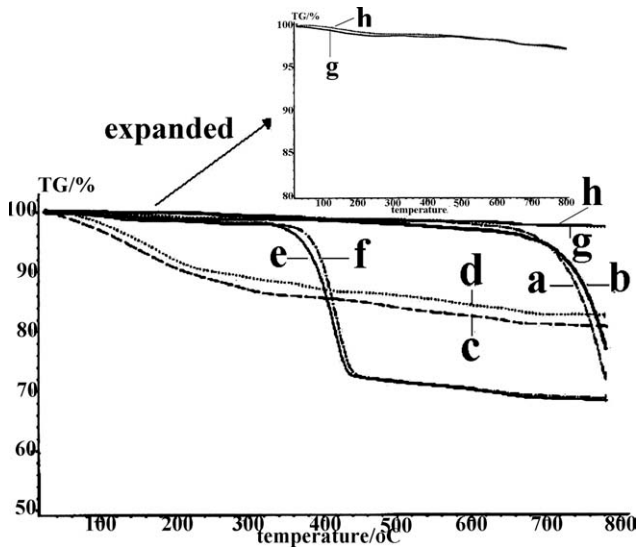

Figure 5 Thermograms of the unmodified and modified fillers: (a) unmodified CC, (b) modified CC, (c) unmodified CS, (d) modified CS, (e) unmodified MH, (f) modified MH, (g) unmodified SF, and (h) modified SF. TG = the % weight loss.

corresponding silanol. These silanol species may have reacted with hydroxyl functional groups on the surface of the fillers and also with neighboring molecules. The reaction of VTES with the surface substrates resulted in a substitution reaction at the silicon and the formation of the silylated surface where the silicon was covalently attached to the surface via an oxygen linkage. Subsequent drying led to the formation of a covalent linkage with the treated surface and the development of the polymeric thin film of silane.

Figure 1 shows the FTIR spectra of the unmodified and modified fillers with VTES. The FTIR spectrum of CC [see Fig. 1(a)] showed the presence of a strong band centered around 1463 cm^{-1}, characteristic of the C—O stretching mode of carbonate, together with a narrow peak around 873 cm^{-1} of the blending mode.[13] Also, the stretching vibrations of the H_2O molecules in the CC occurred at 3456 cm^{-1}. On the spectrum of the treated sample, the fundamental peaks of carbonate could be seen at 1463 and 873 cm^{-1}. Also, the spectrum showed small peaks of —O—Si—O— at 1200–1000 cm^{-1}. In addition, the absorption spectrum of the OH groups at 3436 cm^{-1} decreased. This may have been due to the effectiveness of VTES in reacting with CC. The effectiveness of VTES in reacting with CC impacted its hydrophobic behavior. Also, VTES provided the nonpolar organic substitution with CC, which shielded the polar substrate from interaction with water. This caused the decrease in the absorption spectrum of the —OH groups.

In the FTIR spectrum of the untreated CS [see Fig. 1(b)], the absorption band at 3456 cm^{-1} was attributed to the absorbance of the —OH functional groups of Si—OH in CS, that at 1050 cm^{-1} was due to Si—O stretching, and that at 440–450 cm^{-1} was the silicate chain structure.[14] The modification of CS with VTES increased the intensity peak of the —OH functional groups, which resulted from the silanol groups of VTES. The peaks at 1485 and 1451 cm^{-1} were assigned to $Si—CH_2—CH_3$.

Figure 1(c) shows the FTIR spectra of MH. The O—H stretching bonded with Mg appeared as a sharp peak at 3697 cm^{-1}, and the blending vibration of —OH appeared at 1427 cm^{-1}. For modified MH, its FTIR spectrum was similar to that of the unmodified specimen. However, the intensity peak at 1128 cm^{-1} increased. It showed a characteristic absorption peak of —O—Si—O—. The intensity peak of O—H stretching at 3697 cm^{-1} increased slightly when it was compared with original MH. This resulted from the condensation reaction between MH and VTES. The alkoxy groups of VTES were hydrolyzable groups. After hydrolysis, reactive silanol groups were formed; these could condense with the other —OH groups of MH to form siloxane linkages. At the interface, there was usually only one bond from each silicon of VTES on the substrate surface. The two remaining silanol groups were present in a condensed form. This resulted in an increasing of the intensity peak of —OH groups.

In the FTIR spectrum of unmodified SF [see Fig. 1(d)], the absorption band at 3435 cm^{-1} was attributed to the absorbance of the —OH functional groups of Si—OH in silica; that at 1118 cm^{-1} was due to Si—O stretching. The peak at 805 cm^{-1} was the absorption of Si—O in Si—OH, whereas that at 478 cm^{-1} was the bending vibration absorption of Si—O—Si.[15] The IR spectrum of the treated sample showed all of expected characteristics; the peaks at 1135 and 1095 cm^{-1} were assigned to $Si—O—CH_2—CH_3$.[16]

In general, the aliphatic hydrocarbon substituents in silanes are the hydrophobic entities that enable

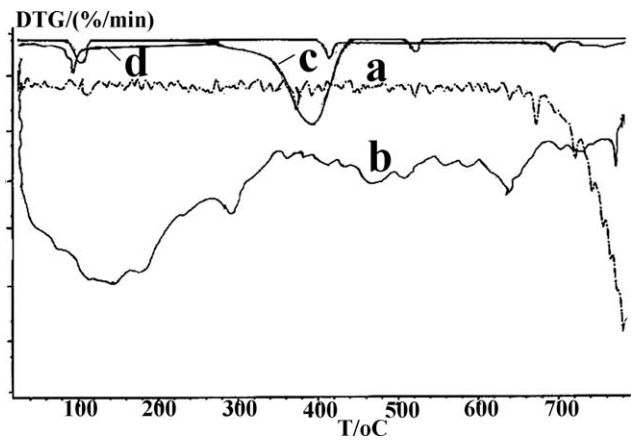

Figure 6 TGA curves of the modified fillers with VTES: (a) CC, (b) CS, (c) MH, and (d) SF. DTG = derivative weight (%/min), T = temperature (°C).

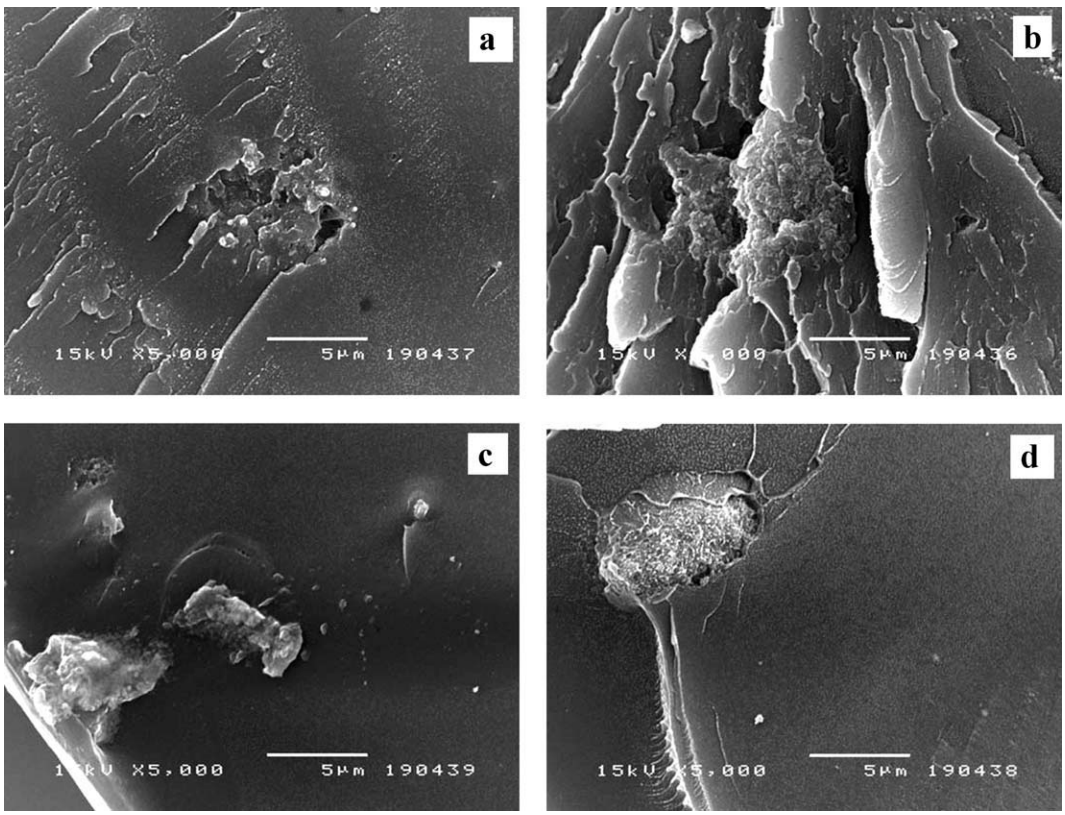

Figure 7 SEM micrographs of the polyester fiber composites: (a) PET/CC, (b) PET/CS, (c) PET/MH, and (d) PET/SF.

silanes to induce hydrophobicity in a modified surface. Thus, the fillers modified with VTES caused their hydrophobic properties. The effectiveness of VTES in reacting with hydroxyls impacted the hydrophobic behavior not only by eliminating the hydroxyls as water-adsorbing sites but also by providing anchor points for the nonpolar organic substitution of VTES, which shielded the polar substrates from interaction with water.

The inorganic fillers in this experiment were hydrophilic in nature. This produced an agglomeration of fillers. The modification of fillers with VTES increased their hydrophobicities. This led to a decrease of the agglomeration of filler particles, as shown in Figures 2–3. As seen in the case of the unmodified fillers, there were particle–particle interactions with a tendency to form aggregates. In the case of SF, it showed a large particle size after treatment with VTES [see Fig. 3(e)]. Hence, it was ball-milled for 30 min at room temperature before it was incorporated into the PET fiber. The SEM micrograph of the surface-modified silica particles obtained after the ball-milling procedure, presented in Figure 3(d), showed that it was composed of small primary particles.

The particle size distribution of the fillers was determined by laser diffraction. The technique of laser diffraction is based on the principle that particles passing through a laser beam will scatter light at an angle that is directly related to their size: large particles will scatter at low angles, whereas small particles will scatter at high angles. The particle size distribution values of the fillers are shown in Figure 4. The results show that the fillers modified with VTES tended to produce a small particle size. This was due to their hydrophobic properties, which led to a decrease in the the agglomeration of filler particles. The statistical analysis revealed that the mean diameter of the modified particles was smaller than that of the unmodified ones (see Table I). The density of the particles shifted from the large particle size to the small one. The mean particle size of the modified particles increased in the order CC $<$ MH $<$ CS $<$ SF. Also, the particle size of the milled SF was smaller than that of SF.

TGA provides a method for the determination of mass change in the material as a function of temperature. The TGA curves of the fillers are presented in Figures 5 and 6. Figures 5(a,b) and 6(a) illustrate the TGA curves of CC. $CaCO_3$ started decomposing around 450°C and showed only one decomposition step. This decomposition must have been due to the conversion of $CaCO_3$ to CaO. The total weight losses of CC and modified CC were 28.32 and 23.26%, respectively.

Figures 5(c,d) and 6(b) show the TGA curves of CS. It was the dehydration of pore water between

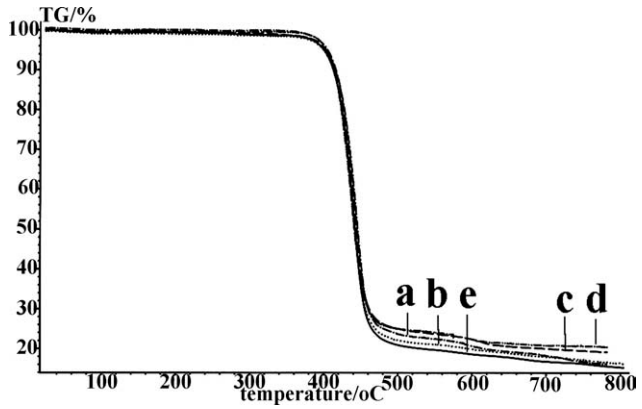

Figure 8 Thermograms of the polyester fiber and polyester fiber composites: (a) PET/CC, (b) PET/CS, (c) PET/MH, (d) PET/SF, and (e) PET. TG = the % weight loss.

particles in the range of 25–100°C. The dehydration of CS hydrates occurred in the temperature range of 100–400°C. The dehydration of calcium hydroxide was observed in the range of 400–600°C. Also, decarbonation of $CaCO_3$ occurred in the temperature range of 600–730°C.[17] The total mass loss of CS and modified CS was 19.32% and 17.64%, respectively.

Figures 5(e,f) and 6(c) show the TGA curves of MH. On the basis of these graphs, the first region of weight loss occurred in the temperature range 40–120°C, which was around 2% correlative to the removal of adsorbed water molecule. The major weight loss happened in the temperature range 300–400°C, with the almost 29% weight loss indicating the decomposition of MH to magnesium oxide. For the temperature regions of about 512–780°C, less than 2% of weight loss took place, and this might have been due to the complete decomposition of $Mg(OH)_2$ to MgO.[18] Following on the TGA thermograms, the total weight losses for the decomposition of MH and modified MH from 40 to 700°C were approximately 31.93 and 31.55%, respectively.

TGAs of SF obtained from 20 to 800°C are shown in Figures 5(g,h) and 6(d). The weight loss curve was almost linear. The first weight loss in the temperature range, 20–120°C, was ascribed to the vaporization of water adsorbed on the particles. Further heating to 800°C resulted in an additional weight loss of 2.84%. This loss was due, in part, to the loss of hydrogen and some carbon.[19] Continued heating resulted in black residues. The TGA data indicated that the mass loss of the surface-modified silica was 2.68%.

As shown in Figure 5, SF had the highest thermal stability. In contrast, MH had the lowest thermal stability of all of the fillers. Given the comparable thermal properties of CC and CS, CC had a better thermal stability than CS. The result shows that the fillers modified with VTES had increased thermal resistance. All of the modified fillers showed remarkable thermal stability, with the mass loss at 300°C being less than 2% for CC, MH, and SF and about 12% for CS. This property would allow them to be melt-blended with high-processing-temperature polymers such as PET.

Effect of the fillers on the spinning of the PET fibers

The undrawn filament in this experiment was spun in a laboratory scale at low speed. It showed a smooth surface with a regular shape. The size of the PET fiber was 1250 μm. It exhibited brittle properties. However, the effect of the filler-containing fibers was examined

The SEM micrographs of the surface-modified fillers in the PET fibers are shown in Figure 7. It was observed that no voids appeared at the interface between the particles and PET matrices. There was good adhesion between the fillers and the matrices. Thus, VTES improved the compatibility between the phases.

TGA was used to study the thermal stability of the PET composites, and the results are listed in Figure 8 and Table I. In Figure 8, it is shown that for PET composites, the temperature of 10% mass loss was virtually unchanged compared to that of virgin PET. When we compared the temperature of 50% mass loss, no marked change was observed between the pure polymer and its inorganic composites; the presence of the fillers appeared to have no marked influence. It was interesting to note that the addition of fillers greatly improved the amount of char, from 15.25% in the case of virgin PET to 16.36, 19.01, and 19.31% for the CS, MH, and SF composites, respectively, which all contained 1% of the inorganic filler. The formation of the char layer prevented oxygen and heat from reaching the PET fibers. It created a thermal insulation barrier between the burning and unburned parts. In addition, it acted to reduce the polymer concentration near the surface and created a less flammable material. Thus, the presence of additives in PET improved its thermal stability. However, the thermal degradation data did not show significant improvement for all of the fillers because the quality of filler used was much lower. The mechanism of the different fillers on the properties of the PET fiber is explained in the following paragraphs.

First, CC started decomposing around 450°C. It released carbon dioxide and calcium oxide on heating. These products revealed the weak combustion. The carbon dioxide produced by the thermal degradation of $CaCO_3$ acted as a diluent of the combustible gases from the thermal degradation of PET. This led to a decrease in the combustible portion of the PET.

Second, the thermal decomposition of CS released water, carbon dioxide, and calcium oxide. Inert gas (water and carbon dioxide) produced by the thermal degradation of CS acted as a diluent of the combustible gases, lowering the oxygen content and slowing the reaction rate of PET during thermal degradation. The role of carbon dioxide was similar to the thermal degradation of CC. Also, CaO formed a char layer on the burning material's surface. This kept oxygen and heat from reaching it.

Third, MH broke down endothermically when it was subjected to high temperature. The decomposition of MH produced water and magnesium oxide. The reaction removed heat from the surroundings, thus cooling the PET during thermal degradation and slowing burning. The water (steam) formed a layer of nonflammable gas near PET's surface, inhibiting flame. In addition, magnesium oxide formed a protective, nonflammable char layer on the PET surface. The protective char layer provided thermal insulation. This caused an increase in the thermal degradation of PET.

The last one was SF. It contributed to the heat resistance of PET by forming a nonflammable char layer on the surface of the burning material. The char layer slowed the heat transfer to unburned PET.

CONCLUSIONS

Inorganic fillers, including CC, CS, MH, and SF, were modified with VTES at room temperature. VTES was an effective surface-modifying agent and improved the particle size distribution, hydrophobicity, and heat-resistance properties. In addition, PET fiber composites were produced. The incorporation of the modified fillers into PET improved its thermal properties. Also, the thermal degradation of the composites depended on the type of filler. All of the results indicate that these fillers were good candidates for use as additives in PET for future applications in heat-resistant materials.

References

1. Haese, M.; Goderis, B.; Puyvelde, P. V. Macromol Mater Eng 2011, 296, 28.
2. Morreale, M.; Dintcheva, N. T.; Mantia, F. P. L. Polym Int 2011, 60, 1107.
3. Fei, G.; Wang, Q.; Liu, Y. Fire Mater 2010, 34, 407.
4. Dorigato, A.; Pegoretti, A. Polym Int 2010, 59, 719.
5. Dorigato, A.; Pegoretti, A.; Fambri, L.; Slouf, M.; Kolarik, J. J Appl Polym Sci 2011, 119, 3393.
6. Pradyot, P. Handbook of Inorganic Chemical Compounds; McGraw-Hill: New York, 2003.
7. Elleithy, R. H.; Ali, I.; Ali, M. A.; Al-Zahrani, S. M. J Appl Polym Sci 2010, 117, 2413.
8. Yuan, Q.; Shah, J. S.; Bertrand, K. J.; Misra, R. D. K. Macromol Eng 2009, 294, 141.
9. Taylor, H. F. W. Cement Chemistry; Academic Press: London, 1990.
10. Iler, R. K. The Chemistry of Silica; Wiley: New York, 1979.
11. Ye, L.; Wu, Q.; Qu, B. J Appl Polym Sci 2010, 115, 3508.
12. Vassiliou, A. A.; Bikiaris, D.; Mabrouk, K. E.; Kontopoulou, M. J Appl Polym Sci 2011, 119, 2010.
13. Boke, H.; Akkurt, S.; Ozdemir, S.; Gokturk, E. H.; Saltik, E. N. C. Mater Lett 2004, 58, 723.
14. Yu, P.; Kirkpatrick, R. J.; Poe, B.; McMilan, P. F.; Cong, X. J Am Ceram Soc 1999, 82, 742.
15. Xie, T.; Zhou, Q.; Feng, S.; Wang, X. J Appl Polym Sci 2000, 75, 379.
16. Shieh, V. T.; Liu, C. M. J Appl Polym Sci 1999, 74, 3404.
17. Feuzicana de Souza Aimeida, A. E.; Sichieri, E. P. Mater Res 2006, 9, 1.
18. Yacob, A. R.; Mustajab, M. K. A. A.; Samadi, N. S. World Acad Sci 2009, 56, 408.
19. Costache, M. C.; Heidecker, M. J.; Manias, E.; Wikie, C. A. Poly Adv Technol 2006, 17, 764.